Quasi-elastic scattering of polarized electrons on polarized ^{3}He

B. Blankleider*
TRIUMF, Vancouver, British Columbia, Canada V6T 2A3
and Nuclear Theory Center and Physics Department, Indiana University, Bloomington, Indiana 47405

R. M. Woloshyn
TRIUMF, Vancouver, British Columbia, Canada V6T 2A3
(Received 22 September 1983)

Cross sections and asymmetries for quasi-elastic scattering of longitudinally polarized electrons on polarized ^{3}He are calculated. The model used consists of impulse approximation plus closure approximation to sum over final states. At the quasi-elastic peak the asymmetry is found to be dominated by scattering from the neutron, and judicious choice of target polarization allows sensitivity to either the neutron's electric or magnetic form factor to be maximized. Away from the quasi-elastic peak, the protons contribute to the asymmetry. The protons's contribution is mainly owing to two partial wave channels, one mixed symmetry S state and one D state which have small total probability in the ^{3}He wave function.

I. INTRODUCTION

Quasi-elastic electron scattering has proved to be a valuable probe of nucleon motion inside a nucleus.[1] Up to now spin-averaged cross sections have been measured and recently longitudinal and transverse structure functions have been separated.[2] Such measurements still do not exhaust all the information obtainable by quasi-elastic scattering. Spin-dependent structure functions (measurable by polarized electron scattering on a polarized target) are needed for a complete description. The spin-dependent structure functions reflect the spin dependence of the nucleon's momentum distribution and in ^{3}He they depend significantly on components in the wave function other than the dominant spatially symmetric S state. One of the purposes of the present calculation, therefore, is to explore how polarized electron scattering can be used to probe the subdominant components of the ^{3}He wave function.

Our second motivation is to study the sensitivity of polarized electron-^{3}He scattering to the neutron electromagnetic form factors. Since the ^{3}He is predominantly a spatially symmetric S state, its two protons are mainly in opposite spin states and we expect that in the vicinity of the quasi-elastic peak spin-dependent effects should be determined primarily by scattering from the neutron. If polarized electron asymmetries could be measured ^{3}He could serve as an effective neutron target.

Our model for electron scattering on ^{3}He consists of impulse approximation with a closure approximation[3] to sum over final states. We neglect meson exchange effects and pion production. Although very simple, this model provides a very good description of available spin-averaged cross sections and, we feel, should be a good starting point for a first calculation of spin-dependent effects.

Section II contains the derivation of the cross section for $^3\vec{\mathrm{He}}(\vec{e},e')X$ and of the nuclear structure functions in terms of the nucleon's momentum distribution. The spin-averaged results are well known but, as far as we know, our expressions for the spin-dependent structure functions are new. A complication of the derivation of the spin-dependent quantities is the appearance of cross terms that normally vanish owing to spin averaging.

Using the closure approximation, the structure functions depend only on the nuclear ground state wave function. For ^{3}He we adopt the wave function owing to Afnan and Birrell,[4] who solved the Faddeev equation for a separable expansion of the Reid soft-core potential. In Sec. III we discuss the ^{3}He wave function and, in particular, its decomposition in an L-S coupling scheme (owing to Derrick and Blatt[5]) which allows the isolation of the component for which the two protons have opposite spin. We find that, in this scheme, only two small components of the wave function result in a significant proton contribution to the polarized electron asymmetry.

Results for the spin-averaged ^{3}He(e,e')X cross section are presented in Sec. IV. With one fixed parameter, namely the closure energy (or equivalently the recoil invariant mass), good agreement is found with experimental measurements in the quasi-elastic peak region for a variety of energies and angles. We conclude that the model is sufficiently good to allow meaningful statements to be made about polarization effects.

One of our goals is to see if polarized electron scattering can be useful for determining the neutron's electromagnetic form factors. For this to be the case requires (a) that there be a kinematic region in which the proton contribution to the asymmetry is negligible, and (b) that a way can be found to isolate separately the neutron electric and magnetic form factors. We show in Sec. V A how these conditions can be achieved, first, by using quasi-free kinematics, and secondly, by judiciously choosing the direction in which the target is polarized.

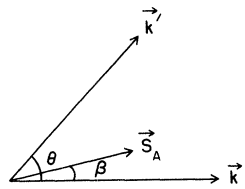

FIG. 1. The scattering plane defined by the ingoing ($\vec{k}$) and outgoing ($\vec{k}'$) electron. The target polarization vector $\vec{S}_A$ is confined to lie within this plane.

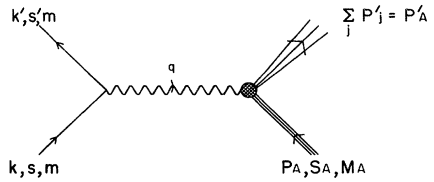

FIG. 2. The Born term for electron-nucleus scattering.

In Sec. V B we discuss (e,e') scattering away from the quasi-elastic peak where scattering from the protons also contributes to the asymmetry. We find that only two channels, one S state and one D state which have only very small probability in the total wave function, play a significant role in determining the protons's contribution to the asymmetry. The asymmetry is largest for electrons of a few hundred MeV and increases as one goes away from the quasi-elastic peak (unfortunately decreasing the cross section at the same time). The polarized electron asymmetry provides a unique probe of the momentum distribution in channels whose effects are normally obscured by the dominant partial wave. Conclusions are presented in Sec. VI.

II. QUASI-ELASTIC SCATTERING

A. Cross section

In this section we present a brief derivation of the inclusive quasi-elastic cross section. Although a number of derivations appear in the literature (see, for example, Refs. 6—8) these do not usually treat the case of polarized initial states. We are interested in the case where the incoming electron is longitudinally polarized and the target's polarization is confined to lie within the scattering plane. This is illustrated in Fig. 1; the scattering angle is θ and the target polarization vector $\vec{S}_A$ makes an angle β with respect to the incoming beam momentum $\vec{k}$.

Before presenting the quasi-elastic case, it is useful to examine (e,e') scattering in general.[9] This will lead us to express the cross section in terms of the four structure functions W_1, W_2, G_1, and G_2. As usual, we limit ourselves to just the one-photon-exchange diagram (Born term). Figure 2 defines the four-momenta, spins, and masses; subscript A refers to the target nucleus, and the components of the four-momenta are $k=(E_k,\vec{k})$, $k'=(E'_k,\vec{k}')$, $P_A=(E_A,\vec{P}_A)$, etc., and $q=(\omega,\vec{q})$.

For inclusive scattering we get[10]

$$d^3\sigma=\frac{4\alpha^2m^2E_A}{q^4FE_{k'}}L^{\mu\nu}W_{\mu\nu}d^3k' , \tag{2.1}$$

where

$$L^{\mu\nu}=\sum_{s'}\bar{u}(k',s')\gamma^\mu u(k,s)\bar{u}(k,s)\gamma^\nu u(k',s') \tag{2.2}$$

is the lepton tensor,

$$W_{\mu\nu}=\sum_{\text{final states}}\frac{(2\pi)^3}{e^2}\int J_\mu(0)J_\nu(0)^*\delta^4(P_f-P_i)\frac{d\vec{P}_{1'}}{(2\pi)^3}\cdots\frac{d\vec{P}_{n'}}{(2\pi)^3} \tag{2.3}$$

is the hadron tensor, J_μ is the hadron current, $F=[(k\cdot P_A)^2-m^2M_A^2]^{1/2}$, α is the fine structure constant, and P_f (P_i) is the total final (initial) four-momentum. In Eq. (2.3) the volume normalizations V have been set equal to 1 as they all cancel in the end. Invariance arguments lead to a representation of the hadronic tensor $W_{\mu\nu}$ by the relation[9]

$$W_{\mu\nu}=\left[-g_{\mu\nu}-\frac{q_\mu q_\nu}{Q^2}\right]W_1+\left[P_{A\mu}+\frac{P_A\cdot q}{Q^2}q_\mu\right]\left[P_{A\nu}+\frac{P_A\cdot q}{Q^2}q_\nu\right]\frac{W_2}{M_A^2}+i\epsilon_{\mu\nu\rho\sigma}q^\rho\left[S_A^\sigma\frac{G_1}{M_A}+\left[P_A\cdot qS_A^\sigma-S_A\cdot qP_A^\sigma\right]\frac{G_2}{M_A^3}\right] , \tag{2.4}$$

where $Q^2=-q^2$ and the structure functions W_1, W_2, G_1, and G_2 depend, in general, on two scalars. A similar expression may be written for the lepton tensor $L^{\mu\nu}$

$$L^{\mu\nu}=\left[-g^{\mu\nu}-\frac{q^\mu q^\nu}{Q^2}\right]\frac{Q^2}{4m^2}+\left[k^\mu-\tfrac{1}{2}q^\mu\right]\left[k^\nu-\tfrac{1}{2}q^\nu\right]\frac{1}{m^2}+i\epsilon^{\mu\nu\rho\sigma}\frac{q_\rho s_\sigma}{2m} . \tag{2.5}$$

Using Eqs. (2.4) and (2.5) in Eq. (2.1) and taking the relativistic limit, we obtain for our choice of beam and target polarization the laboratory inclusive cross section

$$\frac{d^2\sigma}{dE'_kd\Omega'}=\left[\frac{d\sigma}{d\Omega}\right]_{\text{Mott}}\left\{W_2+2\tan^2\frac{\theta}{2}W_1+2\tan^2\frac{\theta}{2}\left[\frac{G_1}{M_A}(E_k\cos\beta+E'_k\cos(\theta-\beta))-2\frac{G_2}{M_A^2}E_kE'_k\right.\right.$$
$$\left.\left.\times(\cos\beta-\cos(\theta-\beta))\right]\right\} , \tag{2.6}$$

where

$$\left[\frac{d\sigma}{d\Omega}\right]_{\text{Mott}}=\frac{\alpha^2\cos^2(\theta/2)}{4E_k^2\sin^4(\theta/2)} . \tag{2.7}$$

The only important assumption made thus far is the validity of the Born approximation for (e,e') scattering. Experimental tests of this assumption could be made by plotting the unpolarized cross section versus $\tan^2(\theta/2)$ keeping Q^2 and ω fixed. This method has been used in elastic scattering where only Q^2 needs to be fixed. We note that a further test may be provided by the spin-dependent part of the cross section; moreover this could be achieved by varying β only.

Having established the general form of the (e,e') cross section, we now choose the quasi-elastic model for the hadron vertex (see Fig. 3). In this model the exchanged photon interacts with just one nucleon (of momentum P, spin S, isospin i, and energy E).

We follow the derivation of Jacob and Maris[8] for the case of electron scattering. The cross section is given by

$$d^9\sigma=\frac{m^2M^2M_A}{FE_{k'}E'E}\frac{1}{(2\pi)^2}$$

$$\times\sum_{\text{final states}}\delta^4(P_f-P_i)\left|\sum_S\mathcal{M}_{\text{eN}}(P,S)g_{A-1,A}^{(S,i)}(\vec{\mathrm{p}})\right|^2$$

$$\times d^3P'_1d^3P'_{A-1}d^3k' , \tag{2.8}$$

where E and E' are the energies of the interacting nucleon before and after collision, respectively;

$$g_{A-1,A}^{(S,i)}(\vec{\mathrm{p}})=A^{1/2}\langle -\vec{\mathrm{P}},S,i\,|\,\langle\phi_{A-1},S_{A-1},i_{A-1}\,|\,\psi_A\rangle \tag{2.9}$$

basically describes the probability of finding a nucleon (of isospin i) with momentum $\vec{\mathrm{P}}$ and spin S, the rest of the nucleus being in the state

$$|\,\psi_{A-1}(M_{A-1})\rangle=|\,\phi_{A-1},S_{A-1},i_{A-1}\rangle , \tag{2.10}$$

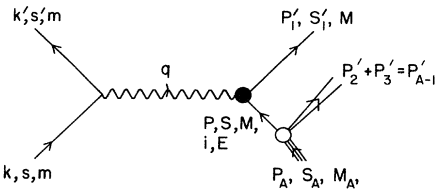

FIG. 3. The quasi-elastic model for ^{3}He(e,e')X used in our calculation.

with internal energy M_{A-1}, spin S_{A-1}, and isospin i_{A-1}. The curious minus sign in Eq. (2.9) arises because for our target wave function ψ_A we use the Jacobi coordinates of Eq. (3.1). $\mathcal{M}_{\text{eN}}(P,S)$ is the invariant electron-nucleon elastic scattering amplitude and is given by

$$\mathcal{M}_{\text{eN}}(P,S)=i\frac{e^2}{q^2}\bar{u}(k',s')\gamma^\mu u(k,s)\bar{u}(P'_1,S'_1)\Gamma_\mu u(P,S) , \tag{2.11}$$

where

$$\Gamma_\mu=\gamma_\mu F_1(q^2)+\frac{i\sigma_{\mu\nu}q^\nu}{2M}\kappa F_2(q^2) \tag{2.12}$$

is the usual nucleon electromagnetic vertex function.

The interacting nucleon is in principle off mass shell; however, practical considerations [e.g., the form factors F_1 and F_2 of Eq. (2.12) are not known for off-shell nucleons] lead us to impose the on-shell condition $E=(\vec{\mathrm{P}}^2+M^2)^{1/2}$. Although some correction can be introduced through the use of an effective mass $M^*\equiv(P_0^2-\vec{\mathrm{P}}^2)^{1/2}$, as done by Mougey *et al.*,[11] it turns out that the on-shell condition is not a bad approximation.

Finally, we note that in Eq. (2.8) the sum over S cannot be taken outside the modulus squared as is done in the spin-averaged case. As we shall see, cross terms in S do, in fact, contribute to the polarized part of the cross section.

B. Quasi-elastic structure functions

In this section we calculate the nuclear structure functions in terms of the nuclear wave functions and the interacting nucleon's own structure functions [introduced shortly, but basically $F_1(q^2)$ and $F_2(q^2)$]. Along the way we introduce the closure approximation used in our calculations.

Comparing Eq. (2.8) with the general form of Eq. (2.1), we find for the quasi-elastic hadron vertex

$$W_{\mu\nu}=\sum_{\psi_{A-1}}\int\frac{M^2}{EE'}\delta^4(P_f-P_i)\sum_{\substack{S,S'\\S'_1}}\bar{u}(P'_1,S'_1)\Gamma_\mu u(P,S)\bar{u}(P,S')\bar{\Gamma}_\nu u(P'_1,S'_1)g_{A-1,A}^{(S,i)}(\vec{\mathrm{P}})g_{A-1,A}^{(S',i)*}(\vec{\mathrm{P}})d^3P'_1d^3P'_{A-1} . \tag{2.13}$$

It is understood that for breakup states of ψ_{A-1}, $d^3P'_{A-1}$ should be replaced by $d^3P'_2d^3P'_3$ ($A=3$); however, we also write $E_{A-1}=(\vec{\mathrm{P}}'^2_{A-1}+M^2_{A-1})^{1/2}$ which for continuum states can be thought of as defining M_{A-1}. It is recognized that the middle term of Eq. (2.13), namely

$$\widetilde{W}_{\mu\nu}^{S,S'} \equiv \sum_{S_1'} \bar{u}(P_1',S_1')\Gamma_\mu u(P,S)\bar{u}(P,S')\bar{\Gamma}_\nu u(P_1',S_1') , \tag{2.14}$$

is a photon-nucleon vertex tensor and should itself be expressible in the form of Eq. (2.4). Indeed, for the diagonal terms we have

$$\widetilde{W}_{\mu\nu}^{S,S} = \sum_{S_1'} \bar{u}(P_1',S_1')\Gamma_\mu u(P,S)\bar{u}(P,S)\bar{\Gamma}_\nu u(P_1',S_1')$$
$$= T_r\left[\Gamma_\mu \frac{\not{P}+M}{2M}\frac{1+\gamma_5 \not{S}}{2}\Gamma_\nu \frac{\not{P}'+M}{2M}\right] , \tag{2.15}$$

and using Eq. (2.12) this evaluates to

$$\widetilde{W}_{\mu\nu}^{S,S} = \left[-g_{\mu\nu}-\frac{q_\mu q_\nu}{Q^2}\right]\widetilde{W}_1 + \left[P_\mu+\frac{P\cdot q}{Q^2}q_\mu\right]\left[P_\nu+\frac{P\cdot q}{Q^2}q_\nu\right]\frac{\widetilde{W}_2}{M^2} + i\epsilon_{\mu\nu\rho\sigma}q^\rho\left[S^\sigma\frac{\widetilde{G}_1}{M}+(P\cdot qS^\sigma - S\cdot qP^\sigma)\frac{\widetilde{G}_2}{M^3}\right] , \tag{2.16}$$

where the nucleon structure functions $\widetilde{W}_1$, $\widetilde{W}_2$, $\widetilde{G}_1$, and $\widetilde{G}_2$ are given by

$$\widetilde{W}_1 = G_M^2\tau , \tag{2.17a}$$

$$\widetilde{W}_2 = \frac{G_E^2+G_M^2\tau}{1+\tau} , \tag{2.17b}$$

$$\widetilde{G}_1 = -\frac{G_M}{2}\frac{G_E+G_M\tau}{1+\tau} , \tag{2.17c}$$

$$\widetilde{G}_2 = \frac{G_M}{4}\frac{G_M-G_E}{1+\tau} , \tag{2.17d}$$

where

$$\tau = \frac{Q^2}{4M^2} , \tag{2.17e}$$

and G_E and G_M are the electric and magnetic form factors of the interacting nucleon, respectively.

The evaluation of the nondiagonal terms of Eq. (2.14) is not so straightforward, but is facilitated by specifically choosing the direction of spin S to be along the quantization axis of the nuclear spin S_A (the z axis). That is, we put $S=u_z$ where u_i ($i=x$, y, and z) is a four-vector, which in the nucleon rest frame is the unit vector in the i direction. The following relations are easily obtained

$$u(P,u_z)\bar{u}(P,-u_z) = \frac{(\not{P}+M)}{2M}\frac{\gamma_5 \not{u}_+}{2} , \tag{2.18a}$$

$$u(P,-u_z)\bar{u}(P,u_z) = \frac{(\not{P}+M)}{2M}\frac{\gamma_5 \not{u}_-}{2} , \tag{2.18b}$$

where $u_+ = u_x + iu_y$, $u_- = u_x - iu_y$. Equation (2.14) then becomes

$$\widetilde{W}_{\mu\nu}^{u_z,-u_z} = \mathrm{Tr}\left[\Gamma_\mu \frac{\not{P}'+M}{2M}\frac{\gamma_5 \not{u}_+}{2}\Gamma_\nu \frac{\not{P}'+M}{2M}\right]$$
$$= i\epsilon_{\mu\nu\rho\sigma}q^\rho\left[u_+^\sigma\frac{\widetilde{G}_1}{M}+(P\cdot qu_+^\sigma - u_+\cdot qP^\sigma)\frac{\widetilde{G}_2}{M^3}\right] , \tag{2.19}$$

since this is just a special case of the step that led from Eq. (2.15) to Eq. (2.16). As expected, we see that the cross terms contribute only to the asymmetry and not to the cross section. A similar relation expresses $\widetilde{W}_{\mu\nu}^{-u_z,u_z}$. Defining

$$\widetilde{A}_{\mu\nu} = \left[-g_{\mu\nu}-\frac{q_\mu q_\nu}{Q^2}\right]\widetilde{W}_1 + \left[P_\mu+\frac{P\cdot q}{Q^2}q_\mu\right]$$
$$\times\left[P_\nu+\frac{P\cdot q}{Q^2}q_\nu\right]\frac{\widetilde{W}_2}{M^2} , \tag{2.20a}$$

$$\widetilde{A}_{i\mu\nu} = i\epsilon_{\mu\nu\rho\sigma}q^\rho\widetilde{A}_i^\sigma , \tag{2.20b}$$

$$\widetilde{A}_i^\sigma = u_i^\sigma\frac{\widetilde{G}_1}{M}+(P\cdot qu_i^\sigma - u_i\cdot qP^\sigma)\frac{\widetilde{G}_2}{M^3} , \tag{2.20c}$$

for $i=x$, y, or z, we have

$$\widetilde{W}_{\mu\nu}^{u_z,u_z} = \widetilde{A}_{\mu\nu}+\widetilde{A}_{z\mu\nu} , \tag{2.21a}$$

$$\widetilde{W}_{\mu\nu}^{-u_z,-u_z} = \widetilde{A}_{\mu\nu}-\widetilde{A}_{z\mu\nu} , \tag{2.21b}$$

$$\widetilde{W}_{\mu\nu}^{u_z,-u_z} = \widetilde{A}_{x\mu\nu}+i\widetilde{A}_{y\mu\nu} , \tag{2.21c}$$

$$\widetilde{W}_{\mu\nu}^{-u_z,u_z} = \widetilde{A}_{x\mu\nu}-i\widetilde{A}_{y\mu\nu} , \tag{2.21d}$$

and Eq. (2.13) becomes

$$W_{\mu\nu} = \sum_{\psi_{A-1}}\int\frac{M^2}{EE'}\delta^4(P_f-P_i)(\widetilde{A}_{\mu\nu}f_0+\widetilde{A}_{x\mu\nu}f_x+\widetilde{A}_{y\mu\nu}f_y$$
$$+\widetilde{A}_{z\mu\nu}f_z)d^3P_1'd^3P_{A-1}' \tag{2.22}$$

where

$$f_0 = |g_{A-1,A}^{(u_z,i)}|^2+|g_{A-1,A}^{(-u_z,i)}|^2 , \tag{2.23a}$$

$$f_x = 2\,\mathrm{Re}(g_{A-1,A}^{(u_z,i)}g_{A-1,A}^{(-u_z,i)*}) , \tag{2.23b}$$

$$f_y = -2\,\mathrm{Im}(g_{A-1,A}^{(u_z,i)}g_{A-1,A}^{(-u_z,i)*}) , \tag{2.23c}$$

$$f_z = |g_{A-1,A}^{(u_z,i)}|^2-|g_{A-1,A}^{(-u_z,i)}|^2 . \tag{2.23d}$$

In Eq. (2.22) only the term $\tilde{A}_{\mu\nu}f_0$ contributes to the non-spin cross section and $f_0=f_0(\vec{P},M_{A-1})$ depends only on the magnitude of $\vec{P}$ and is recognized as the usual spectral function. After integration with respect to P'_1, Eq. (2.22) contains the energy δ function

$$\delta(\omega+M_A-[(\vec{P}+\vec{q})^2+M^2]^{1/2}-(\vec{P}^2+M_{A-1}^2)^{1/2}) ,$$

where we have further changed variables to $\vec{P}=-\vec{P}'_{A-1}$. In order to simplify the calculation we now make use of the closure approximation when performing the sum over the final states ψ_{A-1}. This entails the assumption that most of the contribution comes from states ψ_{A-1} that are clustered in a small energy band around an average value $\bar{M}_{A-1}$. Then replacing M_{A-1} by $\bar{M}_{A-1}$ in the energy δ function enables us to use the closure relation

$$\sum_{\psi_{A-1}} |\psi_{A-1}\rangle\langle\psi_{A-1}| =1$$

when summing the "spectral functions" (2.23) over ψ_{A-1}. We thereby eliminate the states ψ_{A-1} entirely from the problem. The closure approximation is deemed reasonable in view of the two-body nature of the quasi-elastic scattering process and has previously been used with success.[3] Moreover, it is in keeping with the exploratory nature of our investigation.

We denote the "summed spectral functions" with a bar

$$\sum_{\psi_{A-1}} f_i=\bar{f}_i, \quad i=0,x,y,z . \tag{2.24}$$

The evaluation of Eq. (2.22) is further simplified by choosing a coordinate system with the z axis directed along the momentum transfer $\vec{q}$, and by expressing $\vec{P}$ in its spherical coordinates (P,ξ,ϕ). Then $\vec{P}\cdot\vec{q}=Pq\cos\xi$ and an integration over ξ takes care of the remaining energy δ function. We note, however, that the energy conservation relation

$$\omega+M_A-(\vec{P}^2+\vec{q}^{\,2}+2Pq\cos\xi+M^2)^{1/2} -(\vec{P}^2+M_{A-1}^2)^{1/2}=0 \tag{2.25}$$

has solutions (for ξ) only for a limited range R of values of P. Denoting the solution of Eq. (2.25) by ξ_0, where $0\le\xi_0<\pi$, Eq. (2.22) becomes

$$W_{\mu\nu}=\int_0^{2\pi}d\phi\int_R dP\frac{M^2P}{qP^0}\left[\tilde{A}_{\mu\nu}\bar{f}_0+\sum_i\tilde{A}_{i\mu\nu}\bar{f}_i\right]_{\xi=\xi_0} , \tag{2.26}$$

where $P^0=(\vec{P}^2+M^2)^{1/2}$. We identify Eq. (2.26) with the general form, Eq. (2.4), and endeavor to obtain expressions for the hadronic structure functions W_1, W_2, G_1, and G_2. Equating the nonspin parts gives

$$W_1=2\pi\int_R dP\frac{M^2P}{qP^0}\left[\tilde{W}_1+\tfrac{1}{2}\vec{P}^2\sin^2\xi_0\frac{\tilde{W}_2}{M^2}\right]\bar{f}_0(P) , \tag{2.27}$$

and

$$W_2=2\pi\int_R dP\frac{M^2P}{qP^0}\left[\frac{Q^2\vec{P}^2\sin^2\xi_0}{2\vec{q}^{\,2}}+\left[P^0-\frac{P}{q}\cos\xi_0\omega\right]^2\right]\frac{\tilde{W}_2}{M^2}\bar{f}_0(P) . \tag{2.28}$$

Equating the spin parts of Eqs. (2.26) and (2.4) gives

$$S_A^\sigma\frac{G_1}{M_A}+(P_A\cdot qS_A^\sigma-S_A\cdot qP_A^\sigma)\frac{G_2}{M_A^3}=\int_0^{2\pi}d\phi\int_R dP\frac{M^2P}{qP^0}\sum_i\tilde{A}_i^\sigma\bar{f}_i\Big|_{\xi=\xi_0} , \tag{2.29}$$

where $\tilde{A}_i^\sigma$ are given by Eq. (2.20c) and where we choose $S_A=(0,\hat{z})$ to make the calculation of the $\bar{f}_i(\vec{P})$ straightforward. Using the explicit boost expressions for u_i the $\tilde{A}_i^\sigma$ can be expressed in a more practical form

$$\tilde{A}_i^\sigma=\left\{e_0^\sigma\left[\frac{\tilde{G}_1}{M}+P\cdot q\frac{\tilde{G}_2}{M^3}\right]P^i+e_i^\sigma\left[\frac{\tilde{G}_1}{M}+P\cdot q\frac{\tilde{G}_2}{M^3}\right](P^0+M)+P^\sigma\left[P^i\frac{\tilde{G}_1}{M^2}-(P^iq^0-q^i(P^0+M))\frac{\tilde{G}_2}{M^3}\right]\right\}\Big/(P^0+M) , \tag{2.30}$$

where $e_\nu^\mu\equiv\delta_{\mu\nu}$. Now by contracting both sides of Eq. (2.29) with q_σ we eliminate the G_2 term and obtain

$$G_1=2\pi\int_R dP\frac{M_AP}{qP^0}\left[M\bar{f}_z+\left[\frac{P\cos\xi_0}{P^0+M}-\frac{\omega}{q}\right]\sum_i P_i\bar{f}_i\right]\tilde{G}_1\Big|_{\xi=\xi_0} , \tag{2.31}$$

where use was made of Eq. (2.30) and the ϕ integral was trivially done since both $\bar{f}_z$ and $P_x\bar{f}_x+P_y\bar{f}_y$ do not depend on ϕ. Finally, taking the zeroth component of Eq. (2.29) gives

$$G_2=2\pi\int_R dP\frac{M_A^2P}{qP^0}\left[\sum_i P_i\bar{f}_i\frac{\tilde{G}_1}{q}+\left[P^0\bar{f}_z-\frac{P\cos\xi_0}{P^0+M}\sum_i P_i\bar{f}_i\right]\frac{\tilde{G}_2}{M}\right]\Big|_{\xi=\xi_0} . \tag{2.32}$$

III. THE ^{3}He WAVE FUNCTION

The ^{3}He wave function used here is owing to Afnan and Birrell[4] who solved the Faddeev equations in momentum space using as input various separable expansions to the Reid soft-core nucleon-nucleon potential. In particular, the wave function we use corresponds to their unitary pole approximation. For the purpose of discussing our quasi-elastic scattering results, we present a summary of the partial wave decomposition of the wave function.

Assuming three equal mass nucleons with momenta $\vec{k}_1$, $\vec{k}_2$, and $\vec{k}_3$, one can define the Jacobi coordinates $\vec{P}$, $\vec{p}_\alpha$, and $\vec{q}_\alpha$ as follows:

$$\vec{P}=\vec{k}_\alpha+\vec{k}_\beta+\vec{k}_\gamma\ , \tag{3.1a}$$

$$\vec{p}_\alpha=\tfrac{1}{2}(\vec{k}_\beta-\vec{k}_\gamma)\ , \tag{3.1b}$$

$$\vec{q}_\alpha=\tfrac{1}{3}(\vec{k}_\beta+\vec{k}_\gamma-2\vec{k}_\alpha)\ , \tag{3.1c}$$

where (α,β,γ) form a cyclic ordering of the particle labels 1, 2, and 3. $\vec{P}$ is, of course, the momentum of the whole system (from now on taken to be zero), $\vec{p}_\alpha$ is the momentum of particle β in the β-γ center of mass, and $\vec{q}_\alpha$ is the negative of particle α's momentum in the three-body center of mass. Then the three-nucleon wave function

$$\psi(\vec{p}_\alpha,\vec{q}_\alpha)\equiv\langle\vec{p}_\alpha\vec{q}_\alpha\,|\,\psi JM_J TM_T\rangle$$

($J=T=\frac{1}{2}$, $M_T=\frac{1}{2}$ for ^{3}He, $M_T=-\frac{1}{2}$ for ^{3}H) is expressed in terms of partial waves in J-J coupling

$$\psi(\vec{p}_\alpha,\vec{q}_\alpha)=\sum_{N_\alpha,M_{N_\alpha}}(l_\alpha M_{l_\alpha}S_\alpha M_{S_\alpha}\,|\,j_\alpha M_{j_\alpha})(L_\alpha M_{L_\alpha}\sigma_\alpha M_{\sigma_\alpha}\,|\,J_\alpha M_{J_\alpha})(j_\alpha M_{j_\alpha}J_\alpha M_{J_\alpha}\,|\,JM_J)(t_\alpha M_{t_\alpha}\tau_\alpha M_{\tau_\alpha}\,|\,TM_T)$$

$$\times Y_{l_\alpha M_{l_\alpha}}(\hat{p}_\alpha)Y_{L_\alpha M_{L_\alpha}}(\hat{q}_\alpha)\,|\,S_\alpha M_{S_\alpha}\sigma_\alpha M_{\sigma_\alpha}\rangle\,|\,t_\alpha M_{t_\alpha}\tau_\alpha M_{\tau_\alpha}\rangle\langle p_\alpha q_\alpha;\Omega^{TJ}_{N_\alpha}\,|\,\psi\rangle\ , \tag{3.2}$$

where σ_α and τ_α refer to the intrinsic spin and isospin of particle α, l_α is the relative orbital angular momentum of the pair $(\beta\gamma)$, L_α is the orbital angular momentum of the $(\beta\gamma)$ center of mass relative to α, and with the rest of the quantum numbers being defined by

$$\begin{aligned}
&\vec{S}_\alpha=\vec{\sigma}_\beta+\vec{\sigma}_\gamma\ ,\\
&\vec{j}_\alpha=\vec{l}_\alpha+\vec{S}_\alpha\ ,\\
&\vec{j}_\alpha=\vec{L}_\alpha+\vec{\sigma}_\alpha\ ,\\
&\vec{j}=\vec{j}_\alpha+\vec{j}_\alpha\ ,\\
&\vec{t}_\alpha=\vec{\tau}_\beta+\vec{\tau}_\gamma\ ,
\end{aligned} \tag{3.3}$$

and

$$\vec{T}=\vec{t}_\alpha+\vec{\tau}_\alpha\ .$$

The radial part of the wave function, $\langle p_\alpha q_\alpha;\Omega^{TJ}_{N_\alpha}\,|\,\psi\rangle$, may be considered to be the overlap of the state $|\,\psi\rangle\equiv|\,\psi JM_JTM_T\rangle$ with $|\,p_\alpha q_\alpha\rangle$ and $|\,\Omega^{TJ}_{N_\alpha}\rangle$ where

$$|\,\Omega^{TJ}_{N_\alpha}\rangle\equiv|\,(t_\alpha\tau_\alpha)TM_T\rangle\,|\,[(l_\alpha S_\alpha)j_\alpha;(L_\alpha\sigma_\alpha)J_\alpha]JM_J\rangle\ , \tag{3.4}$$

and N_α represents all the α labeled quantum numbers.

Although the partial wave decomposition of Eq. (3.2) is the usual one adopted in constructing a three-body wave function, it does not provide the optimum choice in which to discuss quasi-elastic scattering. Ideally we would like to isolate that part of the ^{3}He wave function which has the two protons in opposite spin states so that they do not contribute to the asymmetry. We expect that this component will be the dominant one in the ^{3}He wave function. The separate terms of Eq. (3.2) do not fulfill this ideal. On the other hand, the partial wave decomposition proposed by Derrick and Blatt[5] admirably suits our purpose. In their scheme L-S coupling is utilized ($\vec{L}=\vec{l}_\alpha+\vec{L}_\alpha$, $\vec{S}=\vec{S}_\alpha+\vec{\sigma}_\alpha$) and moreover, the isospin-spin states $|\,(t_\alpha\tau_\alpha)TM_T\rangle\,|\,(S_\alpha\sigma_\alpha)SM_S\rangle$ are linearly combined to make states of definite symmetry under the interchange of any two particle labels. This is achieved by identifying the states $|\,(S_\alpha\sigma_\alpha)SM_S\rangle$ [or $|\,(t_\alpha\tau_\alpha)TM_T\rangle$] with basis vectors of irreducible representations of the permutation group S_3. In general, a basis vector is written $|\,PK\rangle$ where P takes the values S, A, or M depending on whether the state (and therefore the corresponding irreducible representation) is of "symmetric," "antisymmetric," or "mixed" symmetry, and K (=1 or 2) labels each basis vector within a representation. In the Hilbert space of three identical particles, one of which is in state c (e.g., spin down) the other two being in the same state a (e.g., spin up), the basis states $|\,PK\rangle$ are taken to be

$$\begin{aligned}
|\,S1\rangle&=\frac{1}{\sqrt{3}}(aac+aca+caa)\ ,\\
|\,M1\rangle&=-\frac{1}{\sqrt{6}}(ca+ac)a+\sqrt{2}/3aac\ ,\\
|\,M2\rangle&=\frac{1}{\sqrt{2}}(ac-ca)a\ .
\end{aligned} \tag{3.5}$$

Then the connection with the states $|\,(S_\alpha\sigma_\alpha)SM_S\rangle$ (or $|\,(t_\alpha\tau_\alpha)TM_T\rangle$), enumerated in Table I, is simply

$$|\,(S_\alpha\sigma_\alpha)SM_S\rangle=(-1)^R\,|\,P_\sigma K_\sigma\rangle_{M_S}\ , \tag{3.6}$$

$$[\text{or }|\,(t_\alpha\tau_\alpha)TM_T\rangle=(-1)^R\,|\,P_\tau K_\tau\rangle_{M_T}]\ ,$$

where we have further attached subscripts M_S (or M_T) to

the states $|P_0K_0\rangle$ in order to avoid ambiguities.

The partial wave decomposition of Derrick and Blatt involves states of definite symmetry (S, A, or M) under the simultaneous interchange of particle labels in both spin and isospin coordinates. These states, $|PK\rangle$, are constructed from the individual $|P_\sigma K_\sigma\rangle$ and $|P_\tau K_\tau\rangle$ according to

$$|(P_\tau P_\sigma)PK\rangle = \sum_{K_\tau,K_\sigma} \begin{bmatrix} P_\tau & P_\sigma & P \\ K_\tau & K_\sigma & K \end{bmatrix} |P_\tau K_\tau\rangle\,|P_\sigma K_\sigma\rangle\ , \tag{3.7}$$

where the "3-j" coefficients are tabulated in Ref. 5. The ^{3}He wave function may now be written as

$$\psi(\vec{p}_\alpha,\vec{q}_\alpha)=\sum_{\mathcal{N}_\alpha}\sum_{\substack{M_L,M_S\\ M_{l_\alpha},M_{L_\alpha}}} (-1)^R(LM_LSM_S\,|\,JM)(l_\alpha M_{l_\alpha}L_\alpha M_{L_\alpha}\,|\,LM_L)Y_{l_\alpha M_{l_\alpha}}(\hat{p}_\alpha)Y_{L_\alpha M_{L_\alpha}}(\hat{q}_\alpha)\,|\,(M_\tau P_\sigma)PK\rangle_{M_S}$$
$$\times\sum_{K_\tau,K_\sigma}\begin{bmatrix} M_\tau & P_\sigma & P \\ K_\tau & K_\sigma & K \end{bmatrix}\sum_{j_\alpha,J_\alpha}\begin{Bmatrix} l_\alpha & L_\alpha & L \\ S_\alpha & \sigma_\alpha & S \\ j_\alpha & J_\alpha & J \end{Bmatrix}\langle p_\alpha q_\alpha;\Omega^{TJ}_{N_\alpha}\,|\,\psi\rangle\ , \tag{3.8}$$

where $\mathcal{N}_\alpha=\{L,S\equiv P_\sigma,l_\alpha,L_\alpha,P,K\}$ which we shall refer to as the P-K channels as opposed to the J-J channels labeled by N_α. Implicit in Eq. (3.8) is a transformation from the J-J coupling scheme (in which the wave function is initially given) to the L-S coupling scheme. In Table II we list the possible P-K channels with $l_\alpha+L_\alpha\le 4$, together with their percentage probabilities in our ^{3}He wave function. The restriction to $l_\alpha+L_\alpha\le 4$ defines 98.6% of the wave function, which is totally adequate for our calculations.

TABLE I. Spin states of three nucleons considered as basis vectors ($|P_\sigma K_\sigma\rangle$) or irreducible representations of the symmetry group S_3.

$\lvert(S_\alpha\sigma_\alpha)SM_S\rangle$	$\lvert P_\sigma K_\sigma\rangle_{M_S}$
$\lvert(1\frac{1}{2})\frac{3}{2}\frac{3}{2}\rangle$	$\lvert S1\rangle_{3/2}$
$\lvert(1\frac{1}{2})\frac{3}{2}\frac{1}{2}\rangle$	$\lvert S1\rangle_{1/2}$
$\lvert(1\frac{1}{2})\frac{3}{2}-\frac{1}{2}\rangle$	$\lvert S1\rangle_{-1/2}$
$\lvert(1\frac{1}{2})\frac{3}{2}-\frac{3}{2}\rangle$	$\lvert S1\rangle_{-3/2}$
$\lvert(1\frac{1}{2})\frac{1}{2}\frac{1}{2}\rangle$	$-\lvert M1\rangle_{1/2}$
$\lvert(1\frac{1}{2})\frac{1}{2}-\frac{1}{2}\rangle$	$-\lvert M1\rangle_{-1/2}$
$\lvert(0\frac{1}{2})\frac{1}{2}\frac{1}{2}\rangle$	$\lvert M2\rangle_{1/2}$
$\lvert(0\frac{1}{2})\frac{1}{2}-\frac{1}{2}\rangle$	$-M2\rangle_{-1/2}$

We note that the two $L=0$ channels with the largest probabilities (channels Nos. 1 and 4) have antisymmetric spin-isospin states (and therefore symmetric spatial states) and account for 88.6% [$\equiv P(S)$] of the wave function. In these channels the contribution of the protons to the asymmetry in our model of $^3\vec{\text{He}}(\vec{e},e')X$ is identically zero since interchanging the two protons cannot affect the isospin part of the wave function and it must be that the spin part is antisymmetric. Thus, any contribution of the pro-

TABLE II. The partial wave channels of the three-nucleon wave function within the Derrick-Blatt scheme [Eq. (3.8)].

Channel number	L	S	l_α	L_α	P	K	Probability (%)
1	0	0.5	0	0	A	1	87.44
2	0	0.5	0	0	M	2	0.74
3	0	0.5	1	1	M	1	0.74
4	0	0.5	2	2	A	1	1.20
5	0	0.5	2	2	M	2	0.06
6	1	0.5	1	1	M	1	0.01
7	1	0.5	2	2	A	1	0.01
8	1	0.5	2	2	M	2	0.01
9	1	1.5	1	1	M	1	0.01
10	1	1.5	2	2	M	2	0.01
11	2	1.5	0	2	M	2	1.08
12	2	1.5	1	1	M	1	2.63
13	2	1.5	1	3	M	1	1.05
14	2	1.5	2	0	M	2	3.06
15	2	1.5	2	2	M	2	0.18
16	2	1.5	3	1	M	1	0.37

tons to asymmetry is owing to the small components of the ^{3}He wave function—an observation which forms an important part of our investigation.

IV. THE ^{3}He(e,e′)X DIFFERENTIAL CROSS SECTION

Before considering polarization effects we first need to make sure that the spin-averaged cross sections are adequately described, especially in light of the closure approximation used. The use of the closure approximation results in M_{A-1}, the total energy of the spectator nucleons in the final state, being a parameter of the calculation. We find that the single choice $M_{A-1}=1876$ MeV provides optimal fits to most of the currently available experimental cross sections. That this is the case for a variety of beam energies, energy transfers, and momentum transfers lends support to the use of the closure approximation.

The input to the calculation are the electric and magnetic form factors of the nucleons. For the charge form factor of the neutron we choose the parametrization of Galster *et al.*[12]

$$G_E^n(Q^2)=\frac{-\mu_n^\tau}{(1+\eta\tau)(1+Q^2/B)^2}\ , \tag{4.1}$$

where $B=0.71$ (GeV/c)^2, μ_n is the neutron magnetic moment, and τ is given by Eq. (2.17e). Present indications are that $1\le\eta\le 10$; however, the entire range $0\le\eta\le\infty$ cannot really be excluded. For the other nucleon form factors we use the dipole expressions

$$G_E^p=G_M^p/\mu_p=G_M^n/\mu_n=(1+Q^2/B)^{-2}\ . \tag{4.2}$$

In Fig. 4 we compare our predictions with the data of McCarthy *et al.*[13] and the lower energy data of Hughes *et al.*[14] It is seen that our calculation typically overestimates the peaks and underestimates the cross section in the tails on both sides of the peak. As other calculations give very similar results, we do not expect this to be owing to our use of the closure approximation. Indeed, a comparison with the predictions of Meier-Hajduk *et al.*,[15] who explicitly include two-body and three-body breakup, shows almost identical results. The problem in the high ω tail is mostly understood in terms of meson exchange currents,[16] pion production,[6] and Δ excitations.[17] On the other hand, the reason for the underestimate in the low ω region is not well understood at present and may well be owing to an inadequacy of describing the ^{3}He wave function in terms of nucleons interacting via two-body potentials.[18] Indeed, this region has been attractive for studying the high momentum components of ^{3}He, since arguments about scaling and explicit calculations show that the plane wave impulse approximation is almost exclusively the reaction mechanism.[19] In Sec. V B we shall further investigate this region in terms of the polarization asymmetry. At this stage we conclude that our formalism is able to provide a good enough description of the differential cross sections in order for us to make meaningful statements about polarization effects.

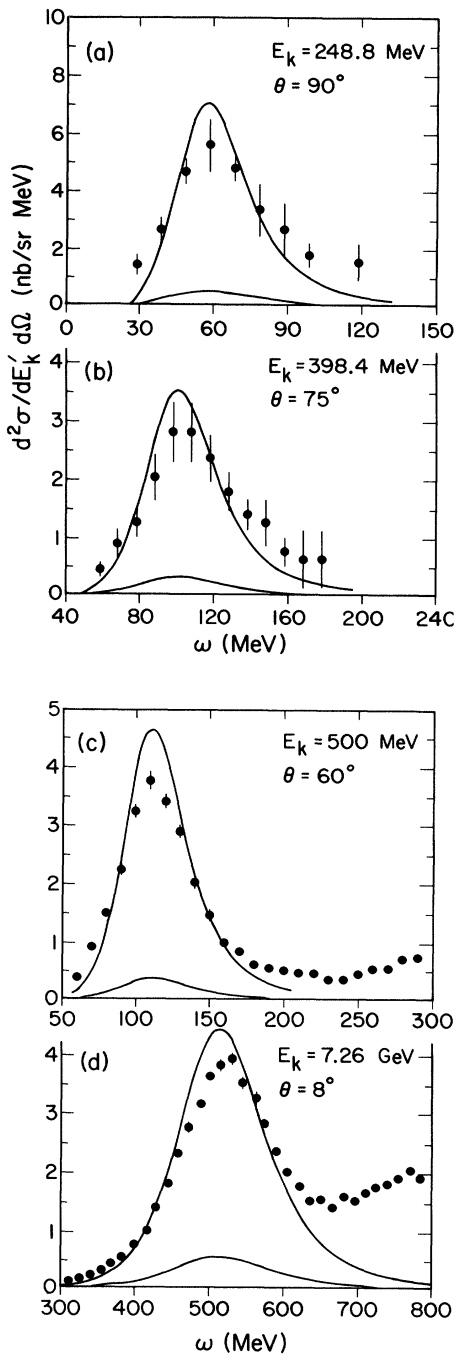

FIG. 4. Differential cross sections for inclusive electron scattering from ^{3}He. The experimental data at $E_k=248.8$ and 398.4 MeV are those of Ref. 14 from which we have chosen only a representative selection. The data at $E_k=500$ MeV and 7.26 GeV are from Ref. 13. The theoretical curves correspond to a closure energy $M_{A-1}=1876$ MeV and we show both the full cross sections and the small contributions owing to quasi-elastic scattering from just the neutron.

V. THE $^3\vec{\text{H}}$e($\vec{\text{e}}$,e)X ASYMMETRY

In this section we discuss the spin-dependent results of our calculation. The central quantity to our discussion is the "longitudinal" asymmetry A defined by

$$A=\frac{\sigma(\theta,\beta,+)-\sigma(\theta,\beta,-)}{\sigma(\theta,\beta,+)+\sigma(\theta,\beta,-)}\ , \tag{5.1}$$

where $\sigma(\theta,\beta,+)$ is the cross section for longitudinally polarized electrons with positive helicity scattering off a target whose polarization lies in the scattering plane and makes an angle β with respect to the beam direction. There are two aspects in which we are particularly interested, namely the sensitivity of the asymmetry to the neutron electric and magnetic form factors, and its dependence on the high momentum components of the ^{3}He wave function. Fortunately they can be studied largely independently by appropriate choice of kinematics.

A. Sensitivity to G_E^n and G_M^n

The fact that the two protons in ^{3}He are mainly in opposite spin states leads to a large cancellation between their contributions to the asymmetry for the $^3\vec{\mathrm{He}}(\vec{e},e')X$ reaction. The remaining contributions come from the neutron and from those protons which are described by the small spatial nonsymmetric components of the wave function. In the vicinity of the quasi-elastic peak even this residual contribution from the protons is suppressed, as here only the S waves of ^{3}He contribute. We therefore expect to get maximum sensitivity to the properties of the neutron in this region. In this section we examine whether one can take advantage of such an arrangement to help determine the neutron electric and magnetic form factors.

From the above observations it is clear that the asymmetry for $^3\vec{\mathrm{He}}(\vec{e},e')X$ at the quasi-elastic peak is basically the asymmetry for a polarized electron scattering on a stationary polarized neutron target scaled by the ratio (at the peak) of the neutron's contribution to the ^{3}He(e,e')X cross section to the total ^{3}He(e,e')X cross section, i.e.,

$$A(\text{peak})\approx A_{\vec{e}\,\vec{n}}\frac{\sigma_{en}}{\sigma_{e^3\mathrm{He}}}(\text{peak})\ . \tag{5.2}$$

$A_{\vec{e}\,\vec{n}}$ is easily calculated using the structure functions (2.17) for the neutron and a version of Eq. (2.6) that has an extra recoil factor

$$\left[1+\frac{2E_k}{M}\sin^2\frac{\theta}{2}\right]^{-1}\ .$$

We shall make use of the approximation (5.2) to interpret some of our results.

We first test the sensitivity of the asymmetry to the neutron electric form factor G_E^n by varying the η parameter of Eq. (4.1), while keeping the other form factors at their values stated in Eq. (4.2). Figure 5 shows the asymmetries at the quasi-elastic peak for $E_k=1.5$ GeV and $\theta=60°$, plotted against the target spin-direction angle β. Both the $^3\vec{\mathrm{He}}$(e,e')X and $\vec{n}(\vec{e},e)$n cases are presented for comparison. As expected, the asymmetries for the two processes are very similar except for their overall magnitude. In general, the ratio $\sigma_{en}/\sigma_{e^3\mathrm{He}}$ does not rise to more than $\sim\frac{1}{4}$ for most kinematical conditions so the asymmetries that are to be expected in $^3\vec{\mathrm{He}}(\vec{e},e')X$ cannot be greater in magnitude than about 0.25. A characteristic of

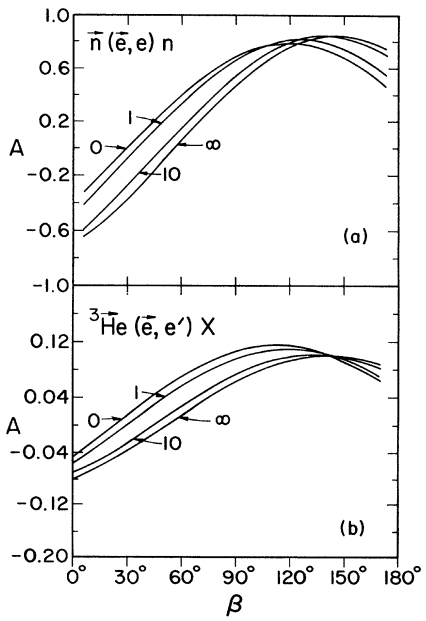

FIG. 5. Asymmetries as a function of target polarization angle β for (a) polarized electron-polarized neutron scattering and (b) inclusive polarized electron scattering from polarized ^{3}He at the quasi-free peak. In both cases $E_k=1.5$ GeV, $\theta=60°$, and the different curves (labeled by values of η) correspond to different choices of the neutron electric form factor [Eq. (4.1)].

the asymmetries in Fig. 5 is that there is a small region of β where the curves crossover, i.e., where the asymmetry essentially does not depend on G_E^n. The approximate crossover point is easily found by demanding, for $\vec{e}$-$\vec{n}$ scattering, that the spin part of the cross section,

$$\frac{d\sigma}{d\Omega}(\text{spin})\sim\frac{G_1}{M}[E_k\cos\beta+E_k'\cos(\theta-\beta)] -\frac{2G_2}{M^2}E_kE_k'[\cos\beta-\cos(\theta-\beta)]\ , \tag{5.3}$$

be independent of G_E^n. This gives

$$\tan\beta=\frac{E_k(E_k'-M)-E_k'(E_k+M)\cos\theta}{E_k'(E_k+M)\sin\theta}\ . \tag{5.4}$$

The results of Fig. 5 are also qualitatively similar to those found in $\vec{e}$-$^2\vec{\mathrm{H}}$ scattering by Cheung and Woloshyn.[20] As in Ref. 20, we note that the asymmetry for different values of G_E^n crosses the $A=0$ axis at significantly separated values of β. As a means of determining G_E^n experimentally, it may prove to be more useful to determine this zero crossing rather than measure the difference in asymmetries at a fixed value of β. The results thus far are at the ω value corresponding to the quasi-elastic peak in the cross section. To show the effects of moving away from the peak, Fig. 6 shows the asymmetry as a function of ω with β fixed at 0° and 60°. The corresponding differential cross section is also shown. Little variation is seen in the asymmetry except in the extreme tails of the cross section where the contribution of the protons is sig-

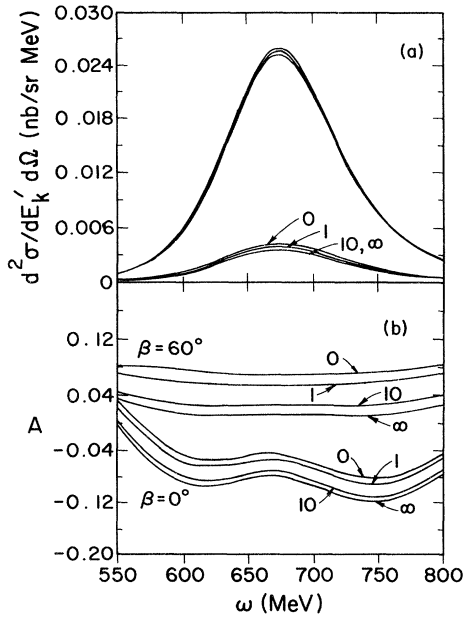

FIG. 6. (a) The differential cross section at $E_k = 1.5$ GeV and $\theta = 60°$ for inclusive electron scattering from ^{3}He as a function of energy transfer ω. (b) The corresponding longitudinal asymmetry for two values of the target polarization angle β. The different curves (labeled by values of η) correspond to different choices of the neutron electric form factor [Eq. (4.1)].

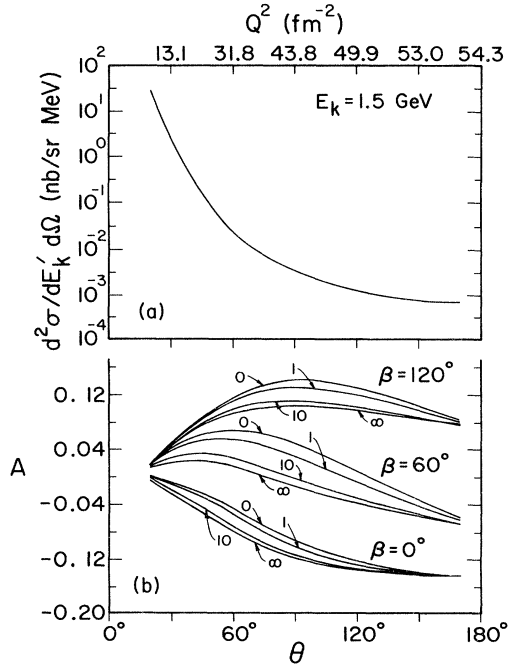

FIG. 7. (a) The differential cross section at the quasi-elastic peak for inclusive electron scattering from ^{3}He as a function of scattering angle θ. The beam energy $E_k = 1.5$ GeV. (b) The corresponding longitudinal asymmetry for three values of the target polarization angle β. The different curves (labeled by values of η) correspond to different choices of the neutron electric form factor [Eq. (4.1)].

nificant. The results for other values of E_k and θ are qualitatively similar to Figs. 5 and 6. In order to summarize these results quantitatively, we show cross sections and asymmetries at the quasi-elastic peak plotted in two ways. The first, Fig. 7, shows variation with respect to θ for fixed E_k, the second, Fig. 8, shows variation with respect to E_k for fixed θ. From both these figures it is seen that the sensitivity to G_E^n, and sometimes the asymmetry itself, increases with θ or E_k, but always at the expense of dropping cross sections.

Besides the practical difficulties of small asymmetries and cross sections, more serious to the proposed determination of G_E^n would be uncertainties brought in by other effects. Foremost of these is the inherent uncertainty in the neutron magnetic form factor G_M^n. Currently it is only known to about 10% at the Q^2 (~ 32 fm^{-2}) corresponding to the quasi-elastic peak region for $E_k = 1.5$ GeV and $\theta = 60°$. We therefore examine the sensitivity of the asymmetry to changes in G_M^n just as we did for G_E^n. Indeed, it would be interesting to see if G_M^n itself could be determined by a measurement of the asymmetry.

To produce a systematic variation in G_M^n we vary the B parameter of Eq. (4.1) around the "standard" value of 0.71 (GeV/c)^2. The choice $B = 0.71 \pm 0.06$ produces changes in G_M^n of about 7% to 13% in the range 10 fm$^{-2} < Q^2 < 60$ fm^{-2}. Again with $E_k = 1.5$ GeV and $\theta = 60°$, we compare the asymmetry for $\vec{n}(\vec{e},e)n$ with the one for $^3\vec{\text{He}}(\vec{e},e')X$ at the quasi-elastic peak (Fig. 9). This time the two are very different. This may seem puzzling at first sight but can readily be understood in terms of Eq. (5.2). Since we can write

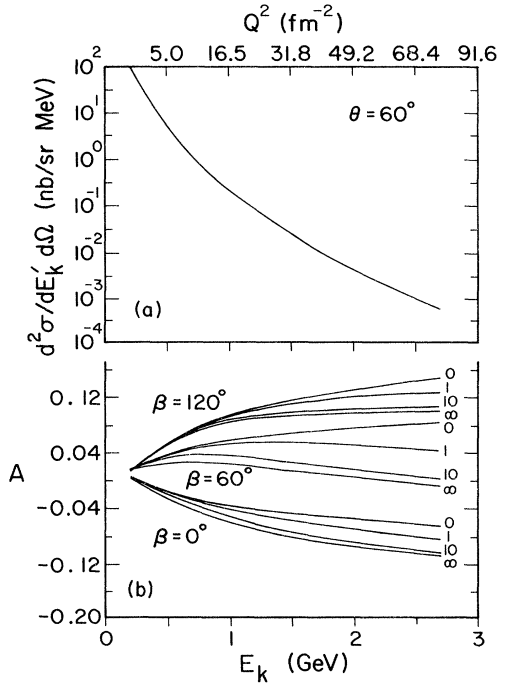

FIG. 8. (a) The differential cross section at the quasi-elastic peak for inclusive electron scattering from ^{3}He as a function of the beam energy E_k. The scattering angle $\theta = 60°$. (b) The corresponding longitudinal momentum for three values of the target polarization angle β. The different curves (labeled by values of η) correspond to different choices of the neutron electric form factor [Eq. (4.1)].

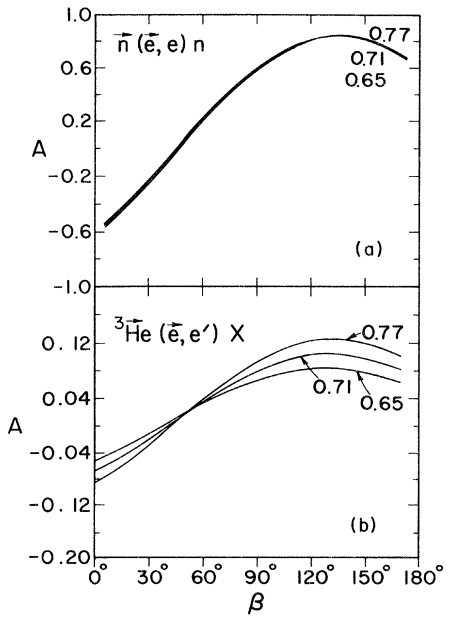

FIG. 9. Asymmetries as a function of target polarization angle β for (a) polarized electron-polarized neutron scattering and (b) inclusive polarized electron scattering from polarized ^{3}He at the quasi-free peak. In both cases $E_k=1.5$ GeV, $\theta=60°$, and the different curves (labeled by values of B) correspond to different choices of the neutron magnetic form factor [Eq. (4.2)].

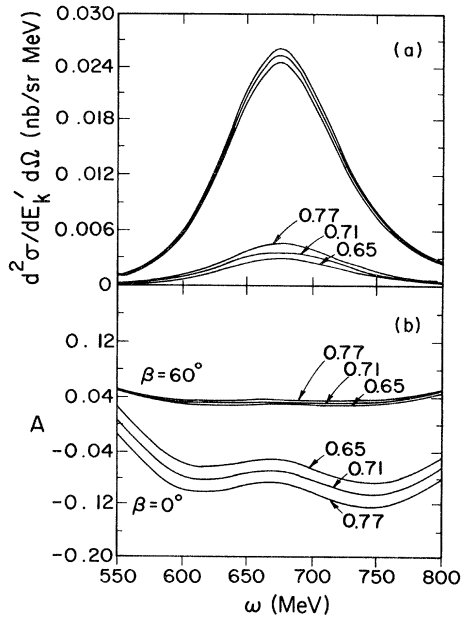

FIG. 10. (a) The differential cross section at $E_k=1.5$ GeV and $\theta=60°$ for inclusive electron scattering from ^{3}He as a function of energy transfer ω. (b) The corresponding longitudinal asymmetry for two values of the target polarization angle β. The different curves (labeled by values of B) correspond to different choices of the neutron magnetic form factor [Eq. (4.2)].

$$A_{\vec{e}\,\vec{n}}=\frac{aG_M^{n^2}+bG_E^nG_M^n}{cG_M^{n^2}+dG_E^{n^2}}\ , \tag{5.5}$$

and G_E^n is a good deal smaller than G_M^n, any variation in G_M^n will tend to cancel between the numerator and denominator, leaving $A_{\vec{e}\,\vec{n}}$ rather insensitive to G_M^n as seen in Fig. 9(a). On the other hand, $A_{\vec{e}^3\vec{\mathrm{He}}}$ also depends on the ratio $(cG_M^{n^2}+dG_E^{n^2})/\sigma_{e^3\mathrm{He}}$ which is sensitive to $G_M^{n^2}$ because of the large contribution of the protons to the denominator. This may be contrasted with the situation when G_E^n is varied. There, just the opposite is the case—$A_{\vec{e}\,\vec{n}}$ is sensitive to G_E^n, while the ratio $\sigma_{en}/\sigma_{e^3\mathrm{He}}$ is not. A feature of Fig. 9(b) that is similar to what was seen when G_E^n was varied is that there is a small range of β for which the asymmetry is essentially independent of G_M^n. Again we can estimate a value of β for which this is so by demanding that the relatively large $G_M^{n^2}$ terms in Eq. (5.3) cancel. This gives

$$\tan\beta=\frac{E_k(E_k'+\tau M)-E_k'(E_k-\tau M)\cos\theta}{E_k'(E_k-\tau M)\sin\theta}\ . \tag{5.6}$$

Comparing Figs. 5(b) and 9(b) shows that one can choose a value of β which at the same time maximizes sensitivity to the form factor of interest (G_E^n or G_M^n) while minimizing any interference from the other form factor. In Fig. 10 we show the cross section and asymmetry as a function of ω, while in Figs. 11 and 12 we present the variation with respect to θ and E_k all for different choices

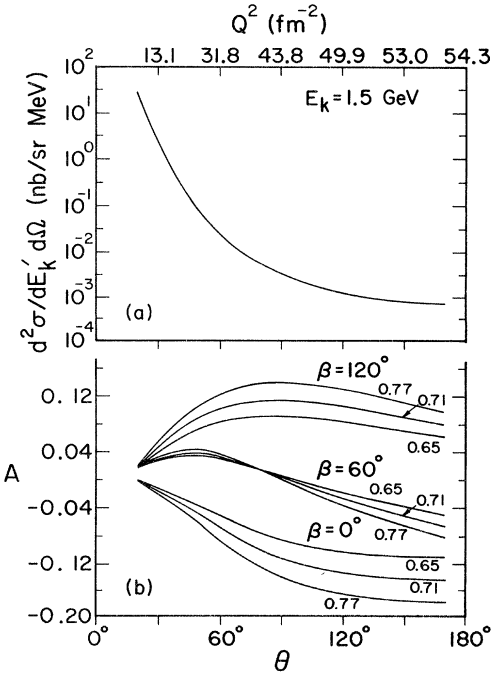

FIG. 11. (a) The differential cross section at the quasi-elastic peak for inclusive scattering from ^{3}He as a function of scattering angle θ. The beam energy $E_k=1.5$ GeV. (b) The corresponding longitudinal asymmetry for three values of the target polarization angle β. The different curves (labeled by values of B) correspond to different choices of the neutron magnetic form factor [Eq. (4.2)].

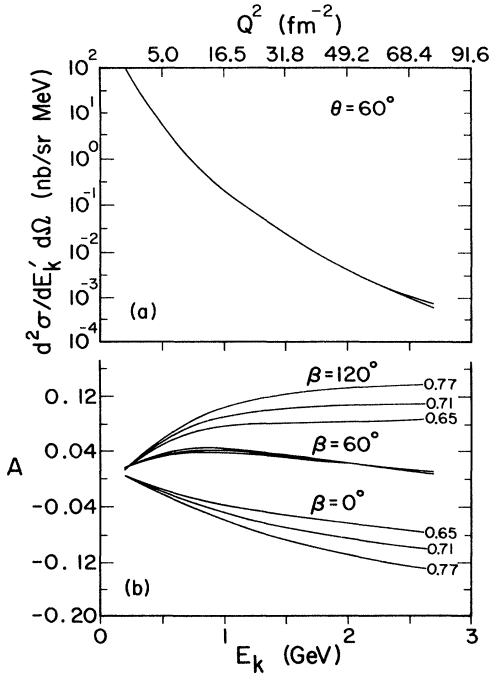

FIG. 12. (a) The differential cross section at the quasi-elastic peak for inclusive electron scattering from ^{3}He as a function of the beam energy E_k. The scattering angle $\theta = 60°$. (b) The corresponding longitudinal asymmetry for three values of the target polarization angle β. The different curves (labeled by values of B) correspond to different choices of the neutron magnetic form factor [Eq. (4.1)].

of the magnetic form factor G_M^n. The same observations can be made about these results as were made about Figs. 6–8 where sensitivity to G_E^n was investigated. A compromise between favorable asymmetries and unfavorable cross sections seems to be inevitable.

B. Sensitivity to the ^{3}He wave function

The origin of the quasi-elastic peak in (e,e') scattering is well established. The peak corresponds to the knocked out nucleon having minimum initial momentum zero. The width of the peak corresponds to the Fermi momentum of the nucleus. In terms of the partial waves in $\psi_{^3\mathrm{He}}$, the peak corresponds to a scattering from S-wave nucleons, while away from the peak, the D waves are expected to contribute (the P waves are small and have negligible effect in any region). It is the S waves that dominate, of course, with the space-symmetric contribution (shown as channel 1 in Table II) being by far the largest at 87% of the wave function. Moreover, as emphasized in Sec. III, the protons in this dominant channel are in opposite spin states and will not contribute to the asymmetry. This elimination of the protons was used in the previous section to look at the properties of the neutron. In this section we turn the problem around and look for nonzero contributions of the protons as a measure of the small spatially nonsymmetric partial waves of ^{3}He (all channels bar 1, 4, and 7 in Table II). Although a nonzero proton contribution to the asymmetry is expected from channel 2 at the quasi-elastic peak (it is truly S wave since $l_\alpha = L_\alpha = L = 0$) and perhaps channel 14 which has $L_\alpha = 0$, the other channels, especially the D waves, can only show their effect where the momenta are high—namely at ω values corresponding to the tails of the quasi-elastic peak.

In order to see the effect of the small partial waves of ^{3}He on the asymmetry, we performed the calculation retaining only a select number of P-K channels from Table II. We note that no restriction is put on the J-J channels N_α in Eq. (3.8) other than that imposed naturally by the limited number of P-K channels. First we find, as expected, that retaining only the spatially symmetric S state (channel 1) already gives almost all the cross section. For the asymmetry we obtain the interesting result that only two of the small channels, the S state ($L_\alpha = 0, l_\alpha = 0$) channel 2, and the D state ($L_\alpha = 2, l_\alpha = 0$) channel 11, contribute significantly. Figure 13 shows the effect of these two channels on the separate neutron and proton contributions to the asymmetry. Channel 1 determines most of the neutron's contribution, while the antisymmetry of the wave function guarantees that the contribution of the protons is identically zero. The effect of channels 2 and 11 on the neutron contribution is minimal. For the protons, these two channels have significant but opposite effects. This explains why, in Fig. 10(b), the asymmetry does not vary a great deal as one moves ω away from the peak

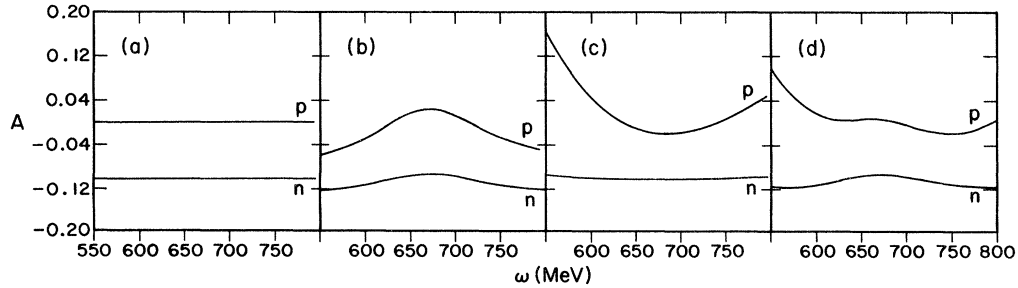

FIG. 13. Contributions of the partial waves of ^{3}He (see Table II) to those components of the asymmetry in $^3\vec{\mathrm{He}}(\vec{e},e')X$ that arise from quasi-elastic scattering off the neutron (n) and proton (p). The kinematics are defined by $E_k = 1.5$ GeV, $\theta = 60°$, and $\beta = 0°$. In (a) only the spatially symmetric S space channel 1 is included, (b) includes channel 1 and the mixed symmetry S state ($L_\alpha = 0, l_\alpha = 0$) channel 2, (c) includes channel 1 and the D state ($L_\alpha = 2, l_\alpha = 0$) channel 11, and (d) includes channels 1, 2, and 11.

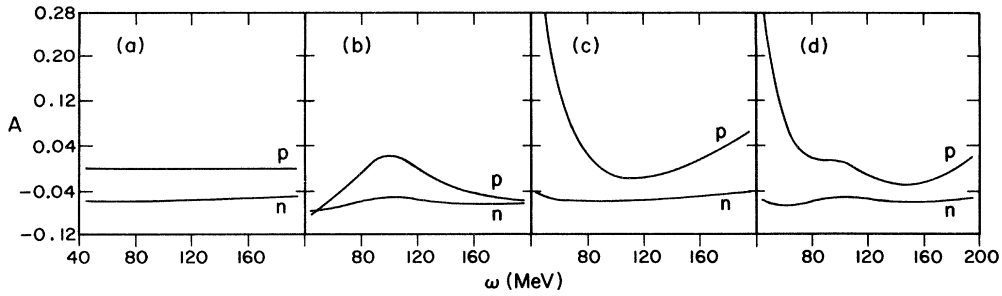

FIG. 14. Same as Fig. 13 except that $E_k = 398.4$ MeV and $\theta = 75°$.

value (although one can see the effect of the D wave in the low energy transfer tail).

We find that the proton contribution to the asymmetry is somewhat larger at lower energies. As an example, Fig. 14 shows results at the energy and angle of the Hughes *et al.*[14] experiment ($E_k = 398.4$ MeV, $\theta = 75°$). The same trends are seen as in Fig. 13 where $E_k = 1.5$ GeV but the asymmetries are, in general, bigger.

Although experimentally what one measures are cross sections, it is interesting to examine the underlying structure functions W_1, W_2, G_1, and G_2 as they isolate much of the physics from the kinematics. Their experimental evaluation may also be possible through a judicious choice of kinematics. Indeed, the use of small angles has already enabled a determination of W_2 at high Q^2 leading to the important scaling behavior.[21] In Fig. 15 we show the structure functions that correspond to the cross section of Fig. 4(b) and asymmetries of Fig. 14 ($E_k = 398.4$ MeV, $\theta = 75°$). For G_1 and G_2 the neutron and proton contributions are shown separately, while for W_1 and W_2 we show the neutron contribution and the full result. Although all the structure functions reflect the presence of the quasi-elastic peak, the proton contributions to G_1 and G_2 are the only ones that do not resemble a Gaussian distribution. The irregularity of these away from the peak is expected and leads to the significant proton contributions to the asymmetry in the tails of the cross section.

It is well known that there is a close relationship between the quasi-elastic cross section and the momentum distribution of the nucleons in the wave function. This is clearly illustrated by the expressions (2.27) and (2.28) for W_1 and W_2 when one recognizes that $\bar{f}_0(p)$ is precisely the momentum distribution. Indeed, the fact that the momentum distribution in a nucleus is largely independent of other properties like the binding energy and form factors, makes quasi-elastic scattering an important tool for studying the nuclear wave function.[7] In a similar way, we expect the asymmetry to be closely connected with the spin-dependent momentum distributions. In their simplest form these distributions are

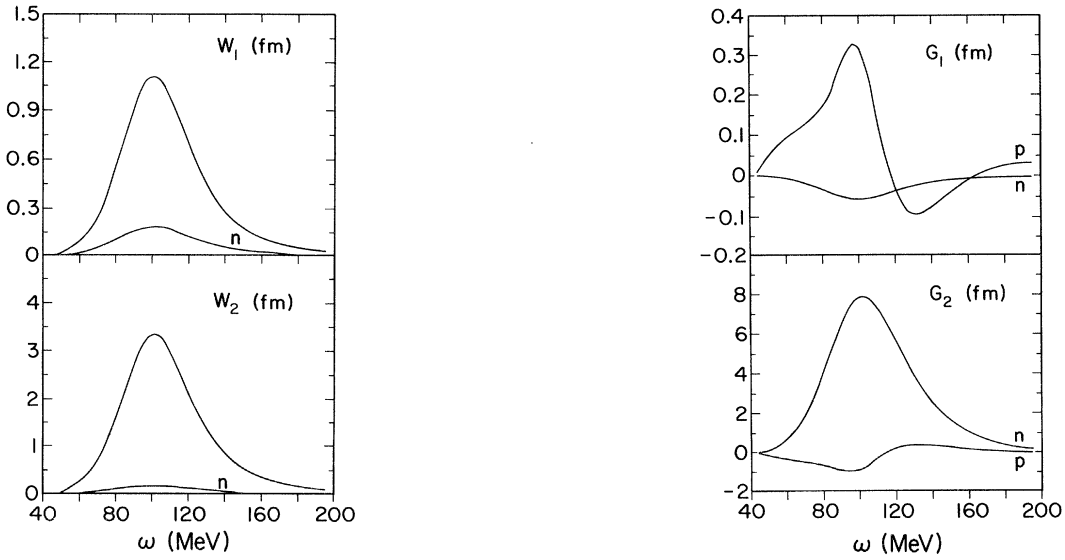

FIG. 15. The structure functions W_1, W_2, G_1, and G_2 for the inclusive scattering of electrons from ^{3}He at $E_k = 398.4$ MeV and $\theta = 75°$. For W_1 and W_2 the contribution of the neutron is shown together with the full result. For G_1 and G_2 only the separate neutron (n) and proton (p) contributions are shown. These structure functions correspond to the cross section of Fig. 4(b) and the asymmetries of Fig. 14.

$$D(\vec{P},\rightarrow)\equiv\sum_{\psi_{A-1}}|g_{A-1,A}^{(u_{z,i})}(\vec{P})|^2, \tag{5.7}$$

describing a nucleon with isospin i and whose spin is parallel to the spin of the nucleus, and

$$D(\vec{P},\leftarrow)\equiv\sum_{\psi_{A-1}}|g_{A-1,A}^{(-u_{z,i})}(\vec{P})|^2, \tag{5.8}$$

describing the nucleon with spin opposite to the spin of the nucleus. In practice there are additional cross terms—see Eqs. (2.23b) and (2.23c). As we have already seen, an advantage that the asymmetry has over the cross section is that it is able to say something about the small components of the ^{3}He wave function. We aim now to illustrate this point in terms of the spin-dependent momentum distributions predicted by our wave function. A slight complication arises in that these distributions depend not only on P as in the spin-averaged case, but also on the azimuthal angle ξ. We choose $\xi=45°$ for our illustration as it is a typical case. Figure 16 shows the proton spin-dependent momentum distributions retaining (a) channels 1 and 2 of the wave function, (b) channels 1 and 11, and (c) all the channels. We note some expected trends: (i) the S wave of mixed symmetry, channel 2, gives the protons of different spin a different distribution even at zero momentum, (ii) the D wave, channel 11, has an effect only at large momentum and then in an opposite way to that of channel 2—an observation already suggested by the asymmetry, (iii) comparing the distributions using the full wave function (c) with the partial ones (a) and (b), we find that from the choice in Table II only channels 2 and 11 contribute to the spin dependence below 1.6 fm^{-1}, a result which again has been noticed in the asymmetry. Above 1.6 fm^{-1} other partial waves contribute to the distributions, but the high momentum makes them difficult to see in the asymmetry. Although $\xi=45°$ is a typical case, it is worth mentioning what happens at other values of ξ. First, we note that the distribution (a) retaining channels 1 and 2 only does not depend on ξ, so only the D-state case (b) need be considered. At $\xi=0$ the probability of finding a proton of nonzero momentum with spin antiparallel to the total spin ($\rightleftarrows$) is larger than finding one with spin parallel ($\rightarrow$). As ξ increases the momentum distributions cross so that at $\xi=90°$ the probability for $\rightarrow$ protons is larger than for $\leftarrow$ protons. Thus, the amount of cancellation between S- and D-wave contributions is controllable to some extent by the kinematics.

For the neutron distribution, Fig. 17, we obtain the expected result that the probability of a neutron having its spin along the direction of ^{3}He's spin is much greater than the reverse. Indeed, the small amount of the $\leftarrow$ component is owing entirely to partial waves other than 1, 2, or 11 and is not noticeable in our results for the asymmetry.

To summarize, we have demonstrated that the nature of the spin-dependent momentum distributions is directly reflected in the asymmetry for $^3\vec{\mathrm{H}}\mathrm{e}(\vec{e},e')X$. We expect that the asymmetry would provide a strong test of theoretical

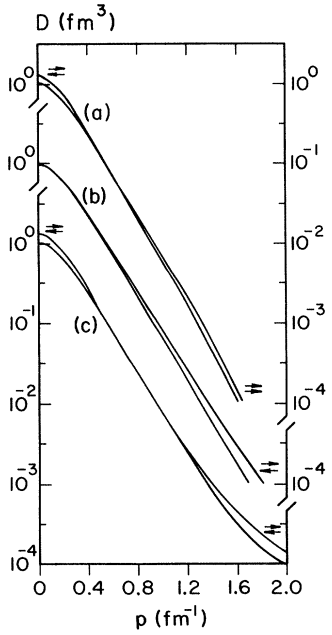

FIG. 16. The proton spin-dependent momentum distributions in ^{3}He for a fixed azimuthal angle of the momentum $\xi=45°$. The curves correspond to a proton with its spin parallel ($\rightarrow$) or antiparallel ($\leftarrow$) to the spin of ^{3}He [see Eqs. (5.7) and (5.8)]. In (a) only the S state ($L_\alpha=0$, $l_\alpha=0$) channels 1 and 2 are included (see Table II). In (b) channel 1 and the D state ($L_\alpha=2$,$l_\alpha=0$) channels 11 are included, while in (c) we include all the channels of Table II.

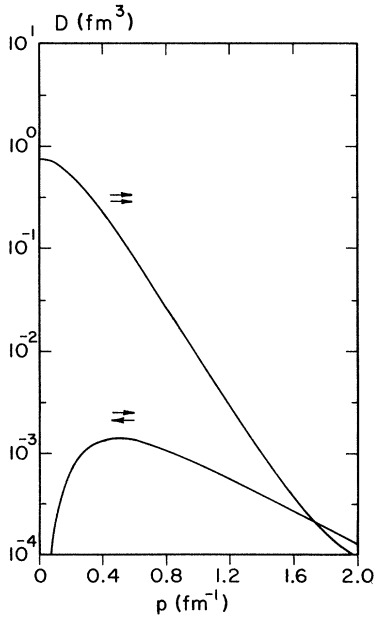

FIG. 17. The neutron spin-dependent momentum distributions in ^{3}He for a fixed azimuthal angle of the momentum $\xi=45°$. The curves correspond to a neutron with its spin parallel ($\rightarrow$) or antiparallel ($\leftarrow$) to the spin of ^{3}He [see Eqs. (5.7) and (5.8)]. All the partial wave channels of Table II are included.

wave functions; in particular, of the two small partial waves. However, before making any final conclusions one needs to test the practicability of such a scheme by comparing predictions of the asymmetry using different three-nucleon wave functions. The difference in wave functions would need to lie, of course, in the momentum distributions. Such a comparison is left for the future.

VI. CONCLUSION

In this paper we studied quasi-elastic scattering of polarized electrons on polarized ^{3}He. Our model consists of impulse approximation along with closure to sum over final states. Using a wave function obtained by solving the Faddeev equation with the Reid soft-core potential and a single fixed value for the closure energy, reasonably good agreement is found for spin-averaged quasi-elastic cross sections for a variety of incident energies and scattering angles.

Near the quasi-elastic peak the contribution of the protons to the asymmetry is very small. Effectively, ^{3}He looks like a neutron target except that the asymmetry is reduced in magnitude owing to the large proton contribution to the spin-averaged cross section (see Fig. 5). The asymmetry at the quasi-elastic peak increases slowly as the incident electron energy is increased from a few hundred MeV to a few GeV (the cross section, however, decreases rapidly).

By choosing the direction in which the ^{3}He target is polarized, it is possible to enhance the sensitivity of the asymmetry at the quasi-elastic peak to either the neutron electric form factor G_E^n or the magnetic form factor G_M^n (compare Figs. 5 and 9). Furthermore, the asymmetry goes through zero as a function of ^{3}He polarization direction precisely in the region where it is least sensitive to uncertainties in G_M^n. The zero crossing of the asymmetry depends essentially only on G_E^n, which could provide a new way of determining this form factor.

As one moves out into the tail of the quasi-elastic peak the contribution of the protons to the asymmetry increases. This contribution depends on the fact that the probability of finding a proton of high momentum in ^{3}He with spin parallel to the total spin is not equal to the probability of having a proton with antiparallel spin. We find that this difference in momentum distributions is determined by only two small components of the ^{3}He wave function, one mixed symmetry S state ($L_\alpha=l_\alpha=0$) and one D state ($L_\alpha=2,l_\alpha=0$). The contributions of these two states to the asymmetry tend to cancel (see Fig. 13). At lower incident electron energies (a few hundred MeV) and at low energy transfer (see Fig. 14) the D-state contribution wins out and the asymmetry approaches 0.3, the largest we have found in any of our calculations. Measurement of the asymmetry in the tail of the quasi-elastic peak would provide a direct test of the spin dependence of the momentum distribution at high momentum which is determined by small components of the wave function and, by implication, of the spin dependence of the short-range force acting between the nucleons.

ACKNOWLEDGMENTS

It is a pleasure to thank I. R. Afnan for providing us with his three-nucleon wave function and helping us with its implementation. We are also grateful to C. Y. Cheung for many helpful discussions and to I. Sick for supplying us with experimental data. This work was supported in part by the Natural Sciences and Engineering Research Council of Canada and by the National Science Foundation.

*Present address: Nuclear Theory Center and Physics Department, Indiana University Bloomington, IN 47405.

[1]R. R. Whitney, I. Sick, J. R. Ficenec, R. D. Kephart, and W. P. Trower, Phys. Rev. C 9, 2230 (1974).

[2]R. Altemus, A. Cafolla, D. Day, J. S. McCarthy, R. R. Whitney, and J. E. Wise, Phys. Rev. Lett. 44, 965 (1980); P. Barreau *et al.*, Nucl. Phys. A402, 515 (1983).

[3]See, for example, F. R. Kroll and N. S. Wall, Phys. Rev. C 1, 138 (1970).

[4]I. R. Afnan and N. D. Birrell, Phys. Rev. C 16, 823 (1977); N. D. Birrell, Ph.D. thesis, Flinders University, 1976, Flinders University Report FIAS-R-12.

[5]G. Derrick and J. M. Blatt, Nucl. Phys. 8, 310 (1958).

[6]E. J. Moniz, Phys. Rev. 184, 1154 (1969).

[7]A. E. L. Dieperink, T. deForest, Jr., I. Sick, and R. A. Brandenburg, Phys. Lett. 63B, 261 (1976); T. deForest, Jr., Ann. Phys. (N.Y.) 45, 365 (1967).

[8]G. Jacob and Th. A. J. Maris, Rev. Mod. Phys. 38, 121 (1966).

[9]For a review, see, F. E. Close, *An Introduction to Quarks and Partons* (Academic, London, 1979).

[10]Throughout we use the conventions of J. D. Bjorken and S. D. Drell, *Relativistic Quantum Mechanics* (McGraw-Hill, New York, 1964).

[11]J. Mougey, M. Bernheim, A. Bussière, A. Gillebert, Phan Xuan Ho, M. Priou, D. Royer, I. Sick, and G. J. Wagner, Nucl. Phys. A262, 461 (1976).

[12]S. Galster, H. Klein, I. Moritz, K. H. Schmidt, D. Wegener, and J. Bleckwenn, Nucl. Phys. B32, 221 (1971).

[13]J. S. McCarthy, I. Sick, R. R. Whitney, and M. R. Yearian, Phys. Rev. C 13, 712 (1976); D. Day, J. S. McCarthy, I. Sick, R. G. Arnold, B. T. Chertok, S. Rock, Z. M. Szalata, F. Martin, B. A. Mecking, and G. Tama, Phys. Rev. Lett. 43, 1143 (1979).

[14]E. B. Hughes, M. R. Yearian, and R. Hofstadter, Phys. Rev. 151, 841 (1966).

[15]H. Meier-Hajduk, Ch. Hajduk, P. U. Sauer, and W. Theis, Nucl. Phys. A395, 332 (1983).

[16]J. W. Van Orden and T. W. Donnelly, Ann. Phys. (N.Y.) 131, 451 (1981).

[17]G. Do Dang, Phys. Lett. 69B, 425 (1977).

[18]I. Sick, in *From Collective States to Quarks in Nuclei, Lecture Notes in Physics 137,* edited by H. Arenhövel and A. M. Sarius (Springer, Berlin, 1981), p. 125.

[19]I. Sick, D. Day, and J. S. McCarthy, Phys. Rev. Lett. 45, 871 (1980).

[20]C. Y. Cheung and R. M. Woloshyn, Phys. Lett. 127B, 147 (1983).

[21]S. Rock *et al.*, SLAC Report SLAC-PUB-2838, 1981 (unpublished).